

Observation of High Recycling Steady H-mode Edge and Compatibility with Improved Core Confinement Mode on JFT-2M

K. Kamiya, H. Kimura, H. Ogawa, H. Kawashima, K. Tsuzuki, M. Sato, Y. Miura and JFT-2M group

Naka Fusion Research Establishment, Japan Atomic Energy Research Institute

E-mail: kamiya@axjft3.tokai.jaeri.go.jp

Abstract. A new operational regime has been discovered on JFT-2M under the boronized first wall condition to produce High Recycling Steady (HRS) H-mode, which is characterized by good energy confinement ($H_{89p} \sim 1.6$) at high density around 70% of the Greenwald density (n_e/n_{GW}), low radiated power fraction, and the complete disappearance of large (Giant) ELMs. Accompanying the HRS H-mode, a coherent magnetic fluctuation is observed at around 50-150kHz, whose characteristics are similar to the Enhanced D_α (EDA) H-mode reported from Alcator C-Mod. The H'-mode, previously observed on JFT-2M, had common features with EDA-mode in terms of the coherent density fluctuation, but it appeared transiently. The HRS operating regime is also similar to EDA-mode, except that HRS is seen even at low q_{95} ($2 < q_{95} \leq 3$). The most important feature of HRS H-mode edge condition is the compatibility with an improved core confinement mode at high density without large ELMs. We have demonstrated that an internal transport barrier (ITB) can be produced with the HRS H-mode edge condition, achieving $\beta_N H_{89p} \sim 6.2$ at the $n_e/n_{GW} \sim 70\%$, transiently.

1. Introduction

Recent experiment in many tokamaks, including ASDEX Upgrade, DIII-D, JET, and JT-60U, have concentrated on advanced scenarios, such as H-mode with type II and grassy ELMs, QH-mode, etc [1-4]. These discharges show a strong reduction of the ELM activity, eliminating pulsed heat loads on the divertor target, and having substantial potential for higher performance by combination of an internal transport barrier (ITB) plus steady H-mode edge. However, it is not well understood which types of advanced H-mode edge condition is more favorable for next-step devices. Also the exact relationship among these different regimes is presently unclear. In the JFT-2M tokamak (major radius $R=1.31\text{m}$, minor radius $a = 0.35\text{m}$, elongation $\kappa \leq 1.7$) [5], an attractive new High Recycling Steady (HRS) operating regime has been discovered after boronization of the first wall of the vacuum vessel. This new regime has following important features, (1) the steady-state H-mode edge condition at high density with good energy confinement, (2) the complete disappearance of Giant ELMs, and (3) the compatibility with ITB.

2. Discovery of High Recycling Steady (HRS) H-mode edge

On JFT-2M, the HRS H-mode edge condition was obtained with co-, counter-, and balance-NBI heating under the strong wall fueling from the boronized first wall and the saturated pumping capability with deuterium gas. Figure 1 (a) and (b) show time history of the co-NBI heating plasmas with $P_{NB} \sim 0.7\text{ MW}$, comparing between before and after boronization at identical experimental conditions ($I_p = 0.2\text{ MA}$, $B_T = 1.3\text{ T}$, and $q_{95} \sim 3.1$). The plasma configuration for these experiments has a standard shape for JFT-2M, with triangularity (δ) ~ 0.4 and elongation (κ) ~ 1.4 . Before boronization (#97009), the plasma made a transition into the standard ELM-free H-mode triggered by a sawtooth crash at $\sim 656\text{ ms}$ as seen by a sharp drop of the D_α signal and increase in the electron density, stored energy, and especially in edge soft X-ray (SXR) intensity passing through just inside separatrix. The radiation loss power (P_{rad}) and core SXR intensity passing through the magnetic axis are also increasing during ELM-free period, showing impurity concentration to the plasma core. And at the onset of second Giant ELM, the plasma makes a back-transition into L-mode. On the other hand, in

the case after boronization (#97156), the plasma behavior exhibits a considerable change from pre-boronization, especially in the impurity, wall pumping and fueling (i.e. recycling rate). As shown in FIG. 1 (b), the radiation loss power is about 1/3 as large as #97009 during Ohmic heating period, resulting in a significant reduction of the threshold power for L/H transition (P_{TH}) to about a half of pre-boronization (P_{TH} at post-boronization ~ 0.4 MW). In this case, although the pumping capability of boronized first wall is saturated with deuterium gas, the plasma makes a transition into the standard ELM-free H-mode at 10 ms after additional heating is applied, as seen by sharp drop in the D_α light and at the same time, both electron density and stored energy begin to rise. But at ~ 625 ms, the plasma makes a second transition into a HRS H-mode, indicating a rise in the D_α signal, which is the source of the name for this operating regime. In contrast to the ELM-free case, the density reaches a new plateau value, and the radiation loss power also stops increasing. The stored energy keeps constant value of ~ 23 kJ for about 7 time global energy confinement time ($\tau_E \sim 27$ ms), corresponding to the confinement enhancement factor, $H_{89p} \sim 1.5$.

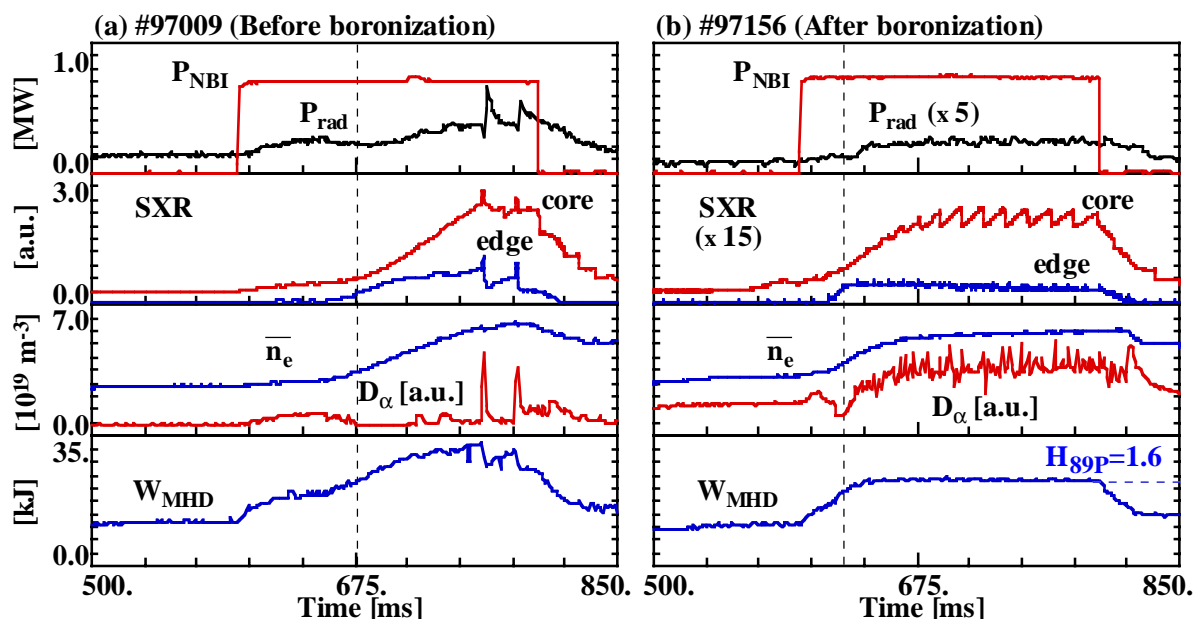


FIG. 1. Time history of the co-NBI heating plasmas with $P_{NB} \sim 0.7$ MW, comparing between (a) before and (b) after boronization at identical experimental conditions ($I_p = 0.2$ MA, $B_T = 1.3$ T, and $q_{95} \sim 3.1$).

Figure 2 (a) and (b) show the spectral time history of the magnetic fluctuation (dB_p/dt) measured by the magnetic probe at the outer midplane. It is noted that two types of small ELMs are seen on top of the enhanced D_α signal, (a) grassy-like and (b) dithering ELMs. As shown in FIG. 2 (a), the coherent mode appears at around ~ 150 kHz after a brief ELM-free period, coincident with the increase in the D_α signal and decrease in dn_e/dt , indicating enhancement in particle transport. It is considered that HRS H-mode may be associated with the coherent fluctuation, which is similar to EDA-mode observed on Alcator C-Mod [6]. The H'-mode, previously observed on JFT-2M [7, 8], had common features with EDA-mode in terms of the coherent density fluctuation, but it appeared transiently.

In this study, the coherent magnetic fluctuations with various frequencies between 50-200kHz have been observed in the different experimental conditions. As shown in FIG. 2 (b), the coherent mode is also seen at around 100kHz. However, its spectrum seems to be made somewhat confusing by the dithering ELMs. The relation among ELMs, coherent-mode, and confinement will be discussed later in this paper.

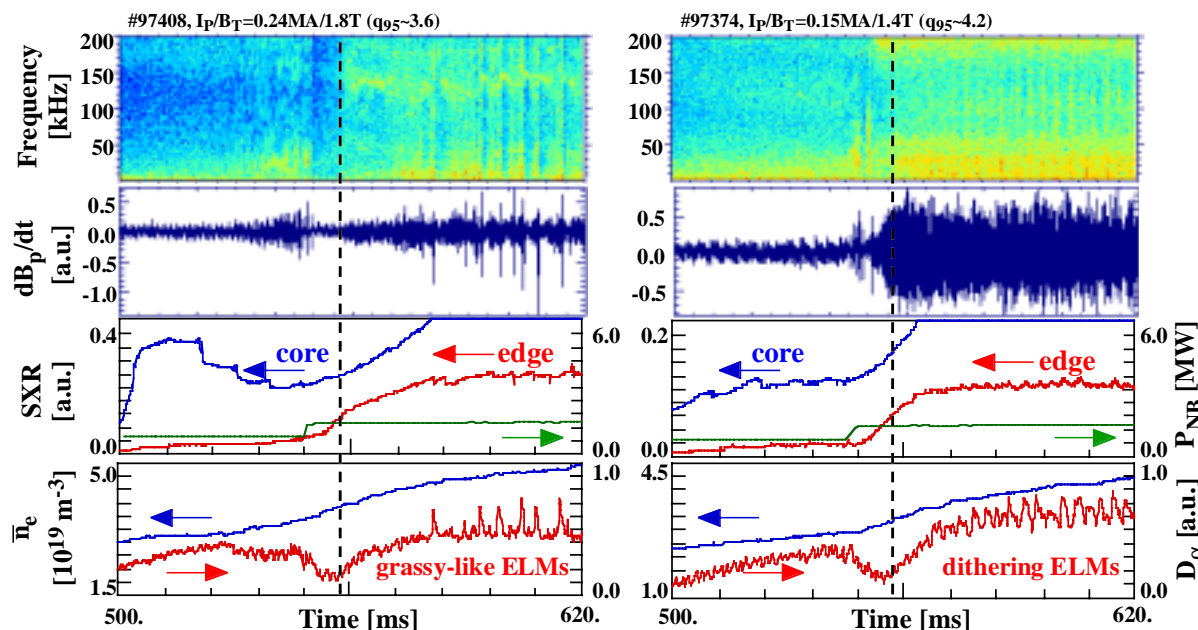


FIG. 2. The spectral time history of the magnetic fluctuation seen during HRS H-mode. Two types of small ELMs are seen on top of enhanced D_α signal, (a) grassy-like and (b) dithering ELMs.

3. HRS H-mode operational space

Even after boronization, the ELMy/ELM-free H-mode is also obtained when the pumping capability of boronized first wall is not saturated. To investigate the condition under which either ELMy or HRS H-modes are obtained, a series of experiments was performed scanning I_p , B_T , (i.e. q_{95}) at fixed triangularity (δ) ~ 0.4 and $P_{NB} \sim 1.4$ MW (balance injection). Most ELMy/ELM-free H-modes are clearly classified as one or the other. But an ambiguity exists near the operational boundary between HRS and other small ELMy regime, namely, A ‘‘Mixture’’ regime. Considering the disappearance of Giant ELMs is one of important features in HRS H-mode, we chose to use the amplitude of ELMs (I_{ELM}) normalized by enhanced D_α level during H-mode (I_{D_α}) as the best indicator (FIG. 3 (a)). Figure 3 (b) and (c) show the results of I_p and B_T scan. It has been found that HRS H-mode is observed widely at q_{95} - I_p and q_{95} - B_T space, although at higher q_{95} (>3.7), no large ELM (i.e. ELMy regime) appears. On the contrary, considerable overlap with the ELMy regime is seen at lower q_{95} (<3.7), except for higher I_p region at ~ 300 kA. Figure 3 (d), (e), and (f) show the operational space of HRS H-mode in relative with the line averaged electron density (n_e), Greenwald fraction (n_e/n_{GW}), and neutral pressure during q_{95} scan described above. It has been found that HRS and ELMy regimes can be separated by n_e/n_{GW} at low q_{95} region, while considerable overlap exists in q_{95} vs. n_e space. Also the mixture regime is seen at HRS/ELMy boundary at $n_e/n_{GW} \sim 0.35$ - 0.45 . In addition, two types of HRS regimes are separated by neutral pressure, indicating that the dithering ELMs are more dominant at higher neutral pressure. As shown in FIG. 3 (g) and (h), it is found that the H_{89p} is slightly degraded as the n_e/n_{GW} increases. It is noted that the H_{89p} value is comparable between ELMy and HRS at same $n_e/n_{GW} \sim 0.4$. But, at higher n_e/n_{GW} around 0.5 - 0.7 , the H_{89p} in the HRS regime with dithering ELMs is systematically lower than the HRS regime with grassy ELMs. Returning to FIG. 2, it is considered that the degradation in the H_{89p} may be connected to the large magnetic fluctuation, which appears slowly after the L/H transition. But the exact causality is still unclear due to lack of data, such as pressure and current profiles at the pedestal. Further understanding is required for obtaining good confinement and steady H-mode without large ELMs.

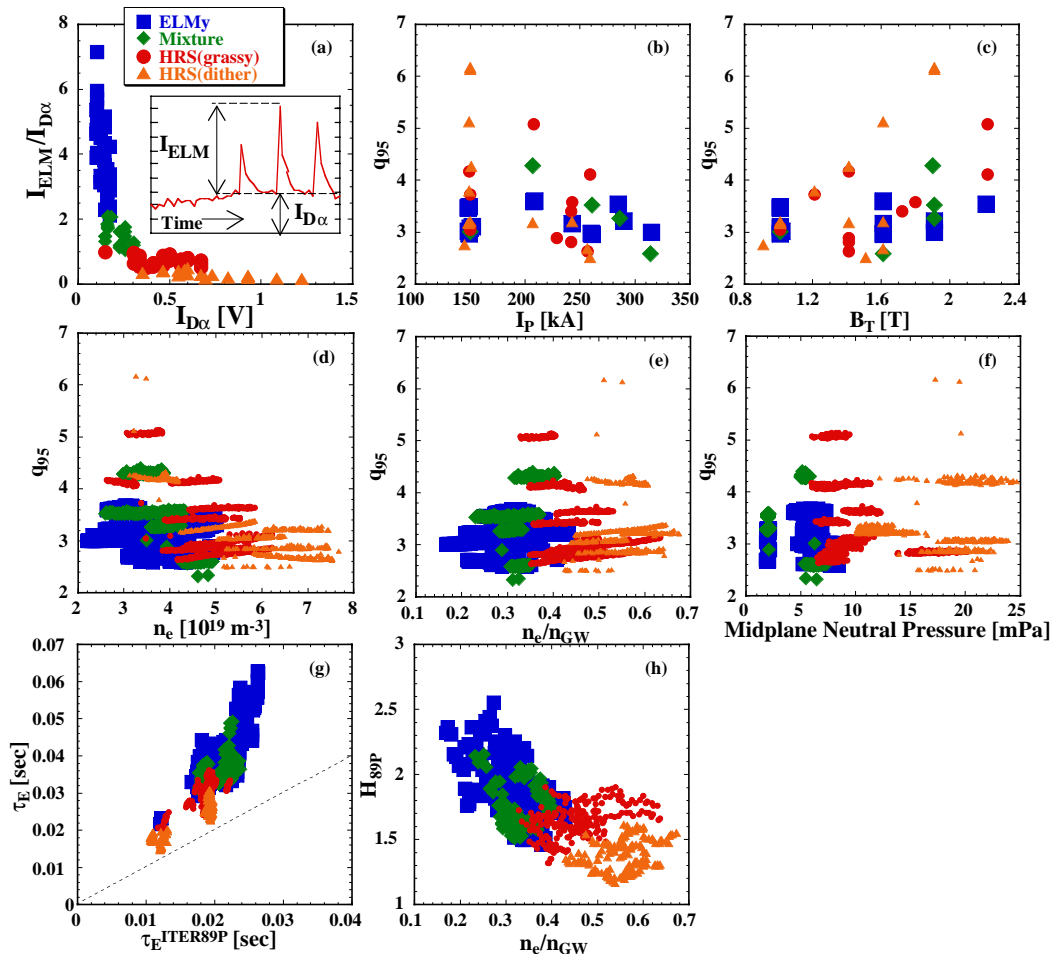


FIG. 3. Results of global parameter scan to determine ELMy/HRS boundary.

4. Compatibility of HRS H-mode edge with Internal transport barrier

Recent experiments on JFT-2M, the discharges having ITB have been produced with steady H-mode edge condition. As shown in FIG. 4 (#97229, $I_p = 0.15$ MA and $B_T = 1.0$ T), the co-NBI with 0.7MW is applied as the pre-heating during I_p -rump-up at 350 ms, and after the plasma current reaches flattop, the ctr-NBI with 0.7MW is added at 450 ms. During the pre-heating phase, the plasma makes a transition into H-mode at ~ 390 ms as seen by a drop in the D_α signal and an increase in the electron density. After a brief ELM-free period, the plasma makes a second transition into the HRS H-mode at ~ 425 ms as seen a rise in the D_α signal and decrease in dn_e/dt . During main-heating phase with balance-NBI of 1.4 MW, the plasma exhibits a bifurcation in the particle and energy confinement from the previous plasma state in the plasma core region, keeping the HRS H-mode edge condition, as seen in continuous increasing in the electron density, SXR (core), and β_N . It is suggested that these confinement improvement results from an ITB formation within the inner half radius (normalized ITB radius, $\rho_{ITB} \sim 0.1-0.2$), which is characterized by the peaked ion temperature profile. The IL-mode, previously observed on JFT-2M [9], has common features with this ITB, except for edge condition (L-mode edge in the previous case). The q-profile also changes from monotonic to zero/weak shear in the plasma core region. It has been found that the HRS H-mode edge is compatible with an improved core confinement mode. Just before collapse, the product $\beta_N H_{89P} \sim 6.2$ ($\beta_N \sim 3.1$, $H_{89P} \sim 2.0$) is achieved at $n_e/n_{GW} \sim 0.7$, transiently. It is believed that combination of an ITB plus steady H-mode edge has substantial potential for higher performance.

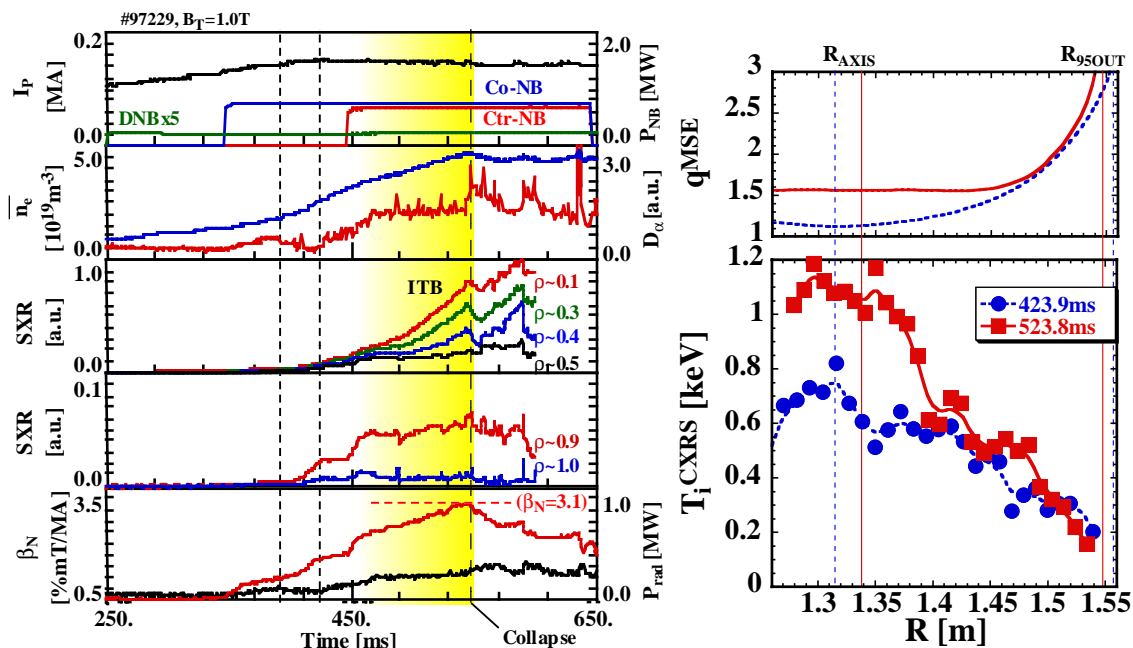


FIG. 4. Time history of ITB plus HRS H-mode discharge (left) and radial profiles of T_i and q (right).

5. Summary

An attractive new ‘‘High Recycling Steady’’ (HRS) operating regime has been discovered on JFT-2M after boronization, where a coherent magnetic fluctuation is associated with its steady-state characteristics. An operational regime is similar to EDA-mode, except that HRS is seen even at low q_{95} ($2 < q_{95} \leq 3$). The most important feature of the HRS H-mode edge condition is the compatibility with an improved core confinement mode at high density without large ELMs. We have demonstrated the product $\beta_N H_{89p} \sim 6.2$ at the $n_e/n_{GW} \sim 70\%$ in a combination of ITB plus HRS H-mode edge condition, transiently.

Acknowledgement

The authors are much indebted to Drs. T. Fujita, T. Fukuda, Y. Kusama, K. Shinohara, H. Takenaga, and T. Takizuka for helpful suggestions and discussions. We would like to thank Dr. M. Bakhtiari for providing the FFT analysis code of the magnetic probe data. We also thank Dr. K. Ida (NIFS) for his careful check of the charge exchange recombination spectroscopy (CXRS) data. Thanks are also due to Drs. A. Kitsunezaki, H. Ninomiya, and M. Kikuchi for continuous encouragement.

References

- [1] Sips, A. C. C., et al., Plasma Phys. Control. Fusion **44**, A151 (2002).
- [2] Greenfield, C. M., Phys. Rev. Lett. **86**, 4544 (2001).
- [3] Becoulet, M. et al., Plasma Phys. Control. Fusion **44**, A103 (2002).
- [4] Kamada, Y., et al., Plasma Phys. Control. Fusion **44**, A279 (2002).
- [5] Ninomiya, H., et al. Fusion Science and Technology **42**, 7 (2002).
- [6] Greenwald, M., et al., Phys. Plasmas **6**, 1943 (1999).
- [7] Shinohara, K., et al., J. Plasma Fusion Res. **74**, 607 (1998).
- [8] Miura, Y., et al., Nucl. Fusion **41**, 973 (2001).
- [9] Miura, Y., et al., Proc.13th Int. Conf. Washington, 1990, Vol.1, IAEA, Vienna 325 (1991).